

# Wafer-Scale Si-Based Metal-Insulator-Semiconductor Photoanodes for Water Oxidation Fabricated Using Thin Film Reactions and Electrodeposition

Shang-Hsuan Wu<sup>1</sup>, Soonil Lee<sup>1</sup>, Yunho Choi<sup>1</sup>, and Edward T. Yu<sup>1\*</sup>

<sup>1</sup> Department of Electrical and Computer Engineering, The University of Texas at Austin, TX, USA

The environmentally friendly generation of hydrogen (H<sub>2</sub>) is anticipated to have a pivotal role in shifting from fossil-based to greener and more sustainable energy systems. Photoelectrochemical (PEC) water splitting is a promising technology for converting solar energy into clean and storable chemical energy and providing carbon-free production of hydrogen for other key applications, e.g., ammonia production. In PEC cells, semiconductors play a key role in absorbing photons from the light source to create mobile charge carriers. Si-based photoelectrodes have drawn much attention due to their moderate bandgap, high charge mobility, long carrier diffusion length, cost-effectiveness, and scalability in manufacturing. To improve the stability of Si-based PEC cells in operation, metal-insulator-semiconductor (MIS) structures have been widely employed [1]. In MIS photoelectrodes, the insulator thickness plays a key role in such MIS photoelectrodes since it influences both efficiency and long-term stability. Photo-generated charges are typically extracted from the semiconductor to the metal catalyst via tunneling through the insulator, mandating the use of extremely thin insulators. However, optimal stability generally motivates the use of thicker insulators.

In this work, we employ a simple and highly scalable method to fabricate high-performance, extremely stable Si-based MIS photoanodes and demonstrate its application to the fabrication of wafer-scale photoanodes. Localized conduction paths formed via an Al/SiO<sub>2</sub> thin-film reaction enable low-resistance charge extraction even through thick insulating layers, and this approach has been shown in our previous work to yield photoanodes with excellent stability [2]. In addition, we demonstrate a two-step Ni/NiFe electrodeposition process to create efficient OER catalysts. The Ni/NiFe catalyst allows for a high Schottky barrier between Si and Ni, lowering the photoanode onset potential, while the NiFe surface layer improves catalytic performance. An unassisted solar-driven water splitting system integrated with wafer-scale photoanode and monocrystalline Si solar cells is demonstrated under both AM 1.5G sunlight simulator and outdoor illumination, with solar-to-hydrogen efficiency of 6.9% achieved with a full-wafer photoanode and minimal optimization.

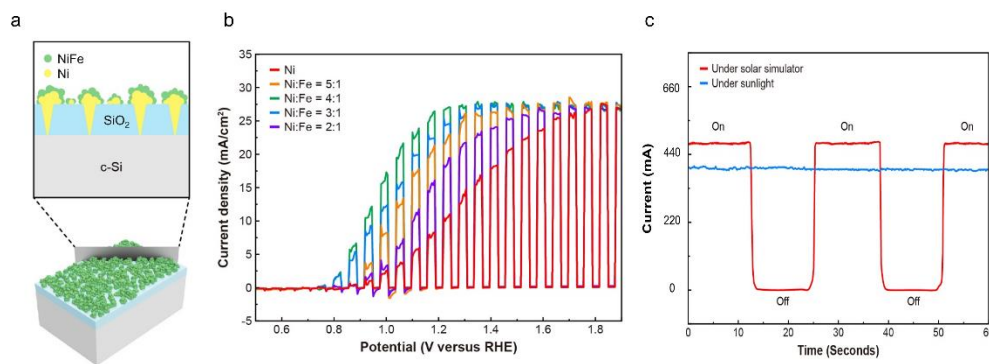


**Figure 1.** (a) Schematic illustrations of the spiked NiFe/Ni/SiO<sub>2</sub>/Si MIS photoanode structures. (b) LSV curves for spiked NiFe/Ni/SiO<sub>2</sub>/Si photoanodes with different Ni:Fe ratios in the NiFe catalyst layers (Ni:Fe = 5:1, 4:1, 3:1, and 2:1). (c) chronoamperometry test of the unassisted solar-driven wafer splitting system under AM 1.5G simulated solar illumination and real outdoor sunlight.

- [1] M. J. Kenney, M. Gong, Y. Li, J. Z. Wu, J. Feng, M. Lanza, H. Dai, *Science*, 342, 6160, 836-840, (2013)  
[2] S. Lee, L. Ji, A. C. De Palma, E. T. Yu, *Nature Communications*, 12, 3982, (2021)

## Supplementary Pages

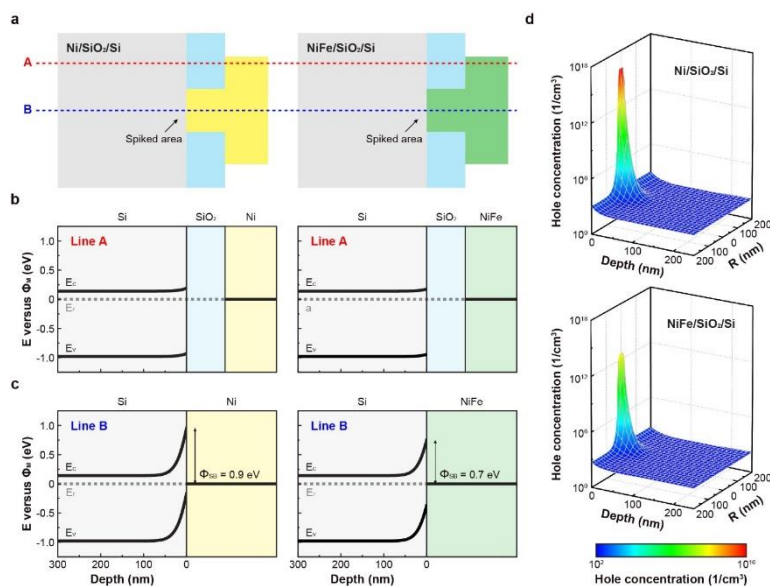


**Figure 2.** Simulations showing potential distributions for different models. (a) Schematic illustration of simulated model structures for MIS photoanodes: Ni/SiO<sub>2</sub>/Si (Model 1) and NiFe/SiO<sub>2</sub>/Si (Model 2) with 90 nm SiO<sub>2</sub> thickness and center spikes. (b, c) Simulated band diagrams at the interface area along the lines labeled in part (a) as A (b) and B (c) for Ni/SiO<sub>2</sub>/Si and NiFe/SiO<sub>2</sub>/Si. (d) Simulated hole concentration near the spiked area for Ni/SiO<sub>2</sub>/Si and NiFe/SiO<sub>2</sub>/Si structures.

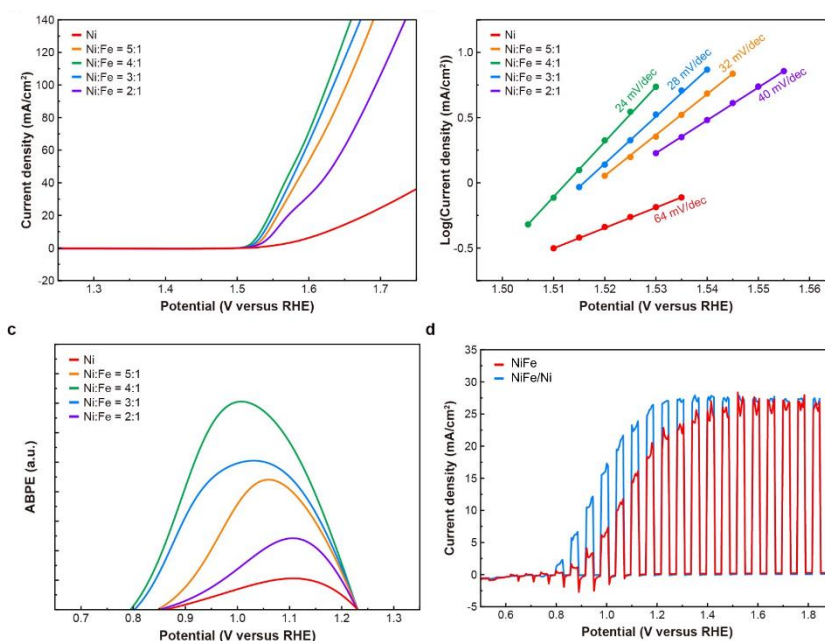


**Figure 3.** PEC characterization of photoanodes for different Ni:Fe ratios. (a) OER polarization curves and (b) Tafel plots for electrodeposited NiFe films on Ni plates in 1 M KOH solution with different Ni:Fe ratios in NiFe alloys (Ni:Fe = 5:1, 4:1, 3:1, and 2:1). (c) normalized ABPE curves for spiked NiFe/Ni/SiO<sub>2</sub>/Si photoanodes with different Ni:Fe ratios in the NiFe catalyst layers (Ni:Fe = 5:1, 4:1, 3:1, and 2:1). (d) LSV curves with chopped illumination in 1 M KOH solutions for the spiked NiFe/SiO<sub>2</sub>/Si and spiked NiFe/Ni/SiO<sub>2</sub>/Si photoanodes (Ni:Fe = 4:1).

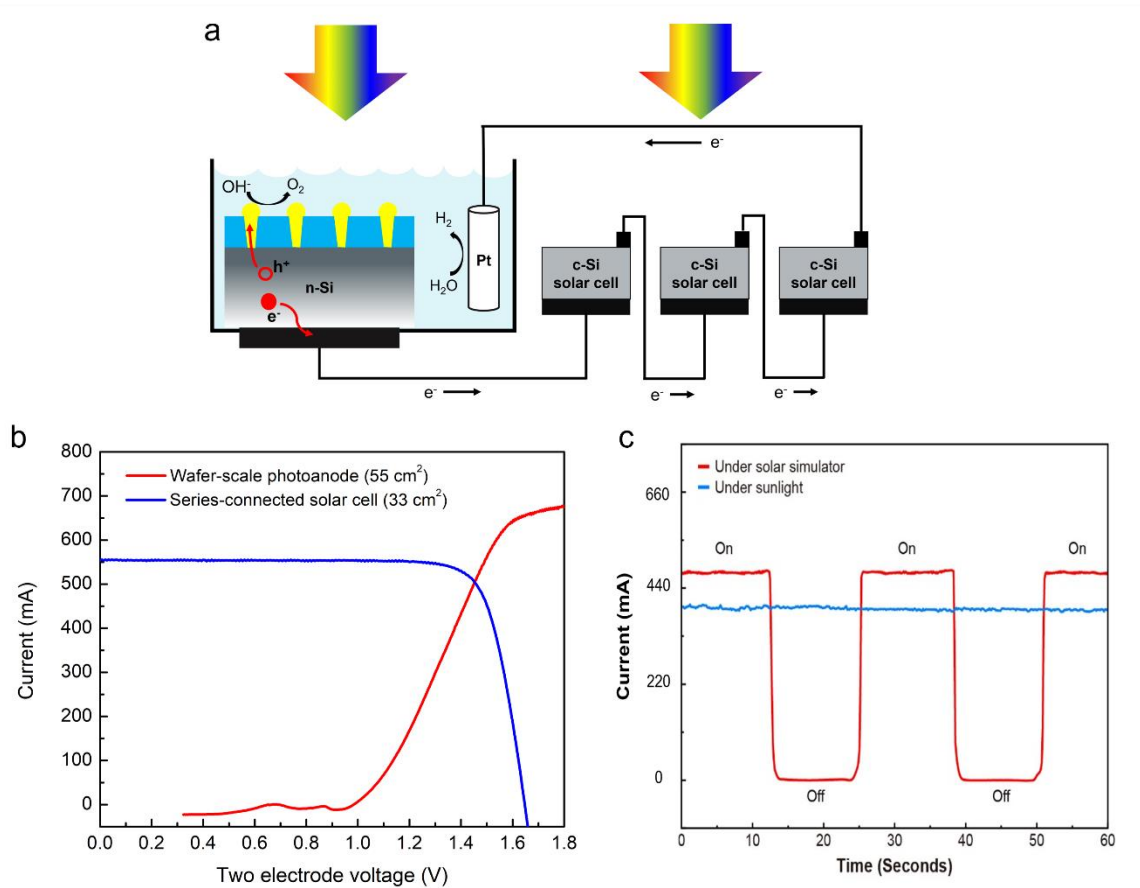


**Figure 4.** PEC performance of unassisted solar-driven water splitting system. (a) Schematics of unassisted water splitting system with wafer-scale photoanode and monocrystalline Si solar cells. (b) I-V curves of monocrystalline Si solar cell and wafer-scale photoanode in a two-electrode system under AM 1.5G illumination. (c) chronoamperometry test of the unassisted solar-driven wafer splitting system under AM 1.5G simulated solar illumination and real outdoor sunlight.